



## City Research Online

### City, University of London Institutional Repository

---

**Citation:** Wang, L., Shen, N., Zhang, M., Fu, F. & Qian, K. (2020). Bond performance of Steel-CFRP Bar reinforced Coral Concrete beams. *Construction and Building Materials*, 245, 118456. doi: 10.1016/j.conbuildmat.2020.118456

This is the accepted version of the paper.

This version of the publication may differ from the final published version.

---

**Permanent repository link:** <https://openaccess.city.ac.uk/id/eprint/23725/>

**Link to published version:** <https://doi.org/10.1016/j.conbuildmat.2020.118456>

**Copyright:** City Research Online aims to make research outputs of City, University of London available to a wider audience. Copyright and Moral Rights remain with the author(s) and/or copyright holders. URLs from City Research Online may be freely distributed and linked to.

**Reuse:** Copies of full items can be used for personal research or study, educational, or not-for-profit purposes without prior permission or charge. Provided that the authors, title and full bibliographic details are credited, a hyperlink and/or URL is given for the original metadata page and the content is not changed in any way.

---

---

---

City Research Online:

<http://openaccess.city.ac.uk/>

[publications@city.ac.uk](mailto:publications@city.ac.uk)

---

# Bond performance of Steel-CFRP Bar reinforced Coral Concrete beams

Lei Wang<sup>a</sup>, Ni Shen<sup>a</sup>, Mingming Zhang<sup>b</sup>, Feng Fu<sup>c\*</sup>, Kai Qian<sup>a</sup>

<sup>a</sup> Guilin University of Technology School of civil and architectural engineering, Guilin 541004, China

<sup>b</sup> Guangxi Beibu Gulf Engineering Research Center for Green Marine Materials, Guilin 541004, China

<sup>c</sup> School of Mathematics, Computer Science and Engineering, City, University of London, London, UK

**Abstract:** Steel-Carbon Fiber Reinforced Polymer (SCFRP) bar provides a new way to solve the shortcomings of poor ductility and low stiffness of FRP reinforced concrete members. In order to understand the bond performance between SCFRP bars and coral concrete, 39 pull-out tests of SCFRP reinforced coral concrete is performed. Different parameters such as the types, diameters and bond lengths of SCFRP reinforcements were investigated. The failure modes, failure mechanism, stress process and bond-slip relationship of the specimens were analyzed. The failure modes of steel bar pull-out can be divided into steel core pull-out before yielding and steel core pull-out after yielding. The concrete splitting failure modes can be divided into coral concrete splitting before steel core yielding and Coral concrete splits after steel core yielding. There are four characteristic points in the bond slip curve: elastic slip point, yield slip point, peak slip point and residual slip point. The bond slip model of SCFRP reinforced coral concrete was developed in this paper using coefficients of slip before steel core yields and slip after steel core yields are 0.86 and 1.0 respectively, which can describe the bond slip behavior between SCFRP and concrete more accurately.

**keywords:** SCFRP bar; coral concrete beam; Pull out test; Bond

## 1. Introduction

Coral concrete casted using coral debris and seawater can solve the problem of material shortage in ocean engineering construction and has high economic value [1-4]. However, marine environment and salt content in coral concrete will accelerate steel corrosion, lead to early deterioration of concrete, reduce the bearing capacity of the structure, and seriously affect the engineering application of coral concrete [5-7]. In order to improve the corrosion resistance of reinforcing bars, the fiber reinforced polymer (FRP), which has the characteristics of corrosion resistance and high tensile strength, is used instead of steel reinforcing bars [8-14], which can effectively solve the engineering failure caused by the corrosion of reinforcing bars. However, research from Bank, L.C [15] and Ovitigala [16] show that FRP bars are brittle materials with low modulus of elasticity, and their components do not have ductility and plastic deformation. When structures fail, the ductility reduction of FRP-concrete members cannot provide early warning, which limits their application in construction.

Steel-Carbon Fiber Reinforced Polymer (SCFRP) bar provides a new way to solve the durability problem caused by steel corrosion and brittle failure caused by low elastic modulus of FRP bars. Nanni and Bakis [17] first tried to wrap reinforcing bars with braided nylon and aramid fabrics and obtained hybrid reinforcement with bilinear stress-strain relationship curve. Inspired by the research on hybrid FRP reinforced concrete structures, Wu [18] proposed production process of Steel-FRP Composite Bars (SFCB) with steel bars as inner core and fibers as outer shell. Because of the addition of steel properties, SFCB have higher elastic modulus. After core yielding, the stress-strain curve shows obvious yielding and good ductility, while retaining the excellent corrosion resistance of FRP material. Ou et al [19] used high strength steel strand as core material to make glass fiber-steel strand composite bars. Their mechanical properties and bond properties were tested. A bond-slip constitutive model of GFRP-steel strand composite bars was proposed.

The bond-slip constitutive relationship between SCFRP bar and concrete is the basis for studying the structural properties of SCFRP bar concrete. Because the shell of SCFRP bar is FRP material, its bond performance is similar to FRP material. At present, the main constitutive models of bond-slip relationship between FRP bar and concrete are as follows: Eligehause [20] proposed a BPE model for bond properties of deformed steel bars in 1983, which has been successfully applied to FRP reinforced concrete by Cosenza et al. and Rosstt et al. [21-22]; Cosenza [23] presumed no horizontal section in bond-slip curve. Malvar [24-25] proposed the bond-slip model between GFRP bars and concrete through a large number of bond tests of FRP bars with different surface finishes. Cosenza and Burong Zhang [26-27] proposed CMR model and Zhang model respectively; Gao [28] summarized the existing bond-slip model and compared it with other models. A large number of test curves show that the existing bond-slip model cannot meet the requirements, so a continuous curve model is proposed. Based on the test results, Xue [29] proposed a bond-slip constitutive relationship model of GFRP bars, which can describe the complete bond-slip curve, and its micro-slip section. The descending section is a straight line and the residual section is a sinusoidal curve. It should be pointed out that although the bond performance between SCFRP bar and concrete is closer to that of FRP bars, Zhang [30] found that the bond behavior of SCFRP bar and concrete before yielding is similar to that of FRP concrete, but the bond-slip failure mode and mechanism between SCFRP bar and concrete are more than that of single material bars. Dong [31] studied the bond durability of SCFRP bar and sea sand concrete in marine environment by using "eccentric pull-out" device. In the existing FRP bond-slip models, the bond behavior of SCFRP bar and concrete after steel core yielding has not been accurately described.

Due to the unique feature of coral concrete materials, the research on the bonding properties of SCFRP reinforced coral concrete are still rare. Therefore, in this paper, pull-out tests of SCFRP bar coral concrete were performed, bond properties and main influencing factors on its bond performance were investigated, a bond curve slip constitutive model which can accurately reflect the bond behavior was developed.

## **2. Test Program**

### ***2.1 Coral concrete preparation***

The coral debris selected in this paper comes from the cleaning products of the South China Sea. Its

mechanical properties are shown in Table 1. The concrete forms are shown in Figure 1(a), (b). The cement is P.O 42.5 grade ordinary Portland cement. The artificial seawater with 3.5% salt content is used for mixing seawater. The water reducing efficiency of the admixture is about 20% with polycarboxylic acid superplasticizer. The quantity is 0.1% of the cement quantity.

**Table 1 Mechanical properties of coral aggregate**

Aggregate	Bulk density ( $\text{kg}\cdot\text{m}^{-3}$ )	Apparent density ( $\text{kg}\cdot\text{m}^{-3}$ )	Porosity (%)	1h water absorption (%)	Cylindrical compression strength (MPa)	Gradation (mm)	Fineness modulus
Coral aggregate	887	1848	52	12	1.82	5~20	—
Coral sand	1370	2690	49	8.7	—	—	2.68

Three kinds of coral concrete with different strength were designed according to the Technical Specification for Light Aggregate Concrete (JGJ 51-2002). The detailed mix ratio and mechanical properties are shown in Table 2.

**Table 2 Mix proportion and mechanical properties of coral concrete**

Concrete grade	Water cement ratio	Cement ( $\text{kg}/\text{m}^3$ )	Coral aggregate ( $\text{kg}/\text{m}^3$ )	Coral sand ( $\text{kg}/\text{m}^3$ )	See water ( $\text{kg}/\text{m}^3$ )	Water reducer ( $\text{kg}/\text{m}^3$ )	Compressive strength (MPa)	Tensile splitting strength (MPa)	Young's Modules (GPa)
C35	0.33	555	823	760	183	0.55	37.73	2.10	28.8



(a) Coral aggregate



(b) Coral sand



(c) SCFRP and CFRP Bar

**Figure 1 Test material**

## 2.2 SCFRP bars

The SCFRP bars have excellent durability due to the existence of inner steel core. The stress-strain relationship curve shows a linear-plastic characteristic with obvious yield point and limit point. The steel core has stable stiffness after yielding, as shown in Figure 2. It shows that it has good ductility and shear

resistance. Unlike the fracture of FRP bars, the yield and ductility characteristics of SCFRP bars are determined by the elastic-plastic properties of steel, and the whole stress process is more stable and reliable. The mechanical properties of composite bars are mainly determined by the properties of fiber materials and steel cores and are affected by bonding surfaces of two different materials.

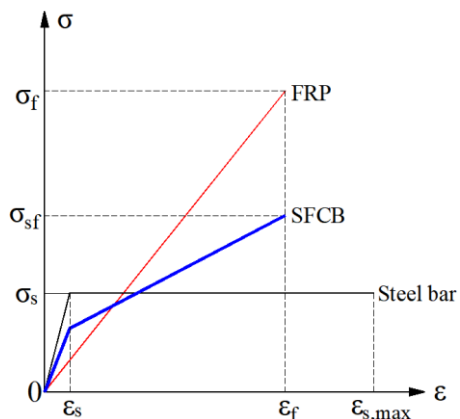


Figure 2 Strain-stress relationship of SFCB

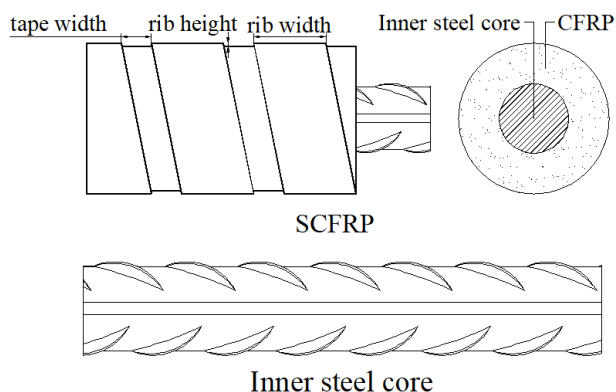


Figure 3 Schematic diagram of SCFRP bars

In this paper, SCFRP bars produced by China Jiangsu Intellectual Science and Technology Nantong Co., Ltd. as shown in Figure 1 (c) are used for the test. The structure sketch is shown in Figure 3, and the main material properties are shown in Table 3.

Table 3 Mechanical properties of rebars

Type of Rebars	SCFRP bar diameter (mm)	Steel core diameter (mm)	Rib height (mm)	Rib width (mm)	Rib spacing (mm)	Yield strength (MPa)	Ultimate strength (MPa)	Rebar Young's Modules (GPa)	Outer fibre Young's Modules (GPa)	Steel core Young's Modules (GPa)
SCFRP	11.45	6	0.50	8.68	10.98	167.8	760.4	126.9	110	200
SCFRP	14.08	6	1.13	6.83	10.15	173.2	1073.8	132.6	110	200
SCFRP	14.10	8	0.68	11.0	13.50	233.7	858.4	136.0	110	200
SCFRP	15.80	10	0.53	13.13	15.25	263.5	881.0	142.3	110	200
CFRP bar	12.12	-	0.7	6.55	8.58	-	1907.6	113.6	-	-

### 2.3 Test specimens

Pull-out test is a classical method to study bond performance between steel bar and concrete. According to Canadian Standards Association (CSA) standard, 39 pull-out specimens with dimensions of 150 \*150 \*150 mm, 200 \*200 \*150 mm were manufactured in this test. The factors such as type of steel bar, diameter of SCFRP bar and bond length were considered respectively. In order to avoid the stress asynchronism between inner steel core and carbon fiber of SCFRP bar at the clamping end, 100 mm long

carbon fiber was stripped at the clamping end, exposes the steel core, and bonds with a 300 mm long steel sleeve. 10 mm long carbon fiber was also stripped at free end of the SCFRP bars to facilitate the bond slip measurement. The relative slip of steel core and carbon fiber is measured, as shown in Figure 4. The specimens were number as AB-C, A represents the type of reinforcement (S represents SCFRP-coral concrete specimens, C represents CFRP bars-coral concrete specimens), B represents the diameter of composite bars (steel core diameter), C represents the bond length.

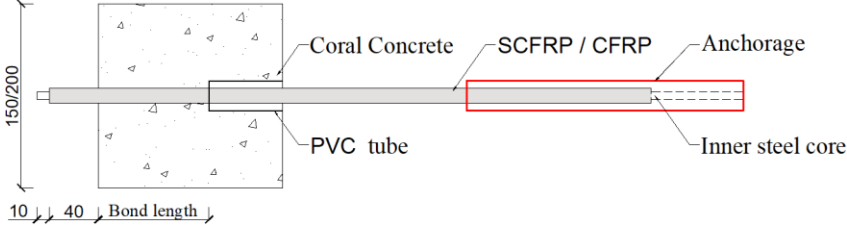
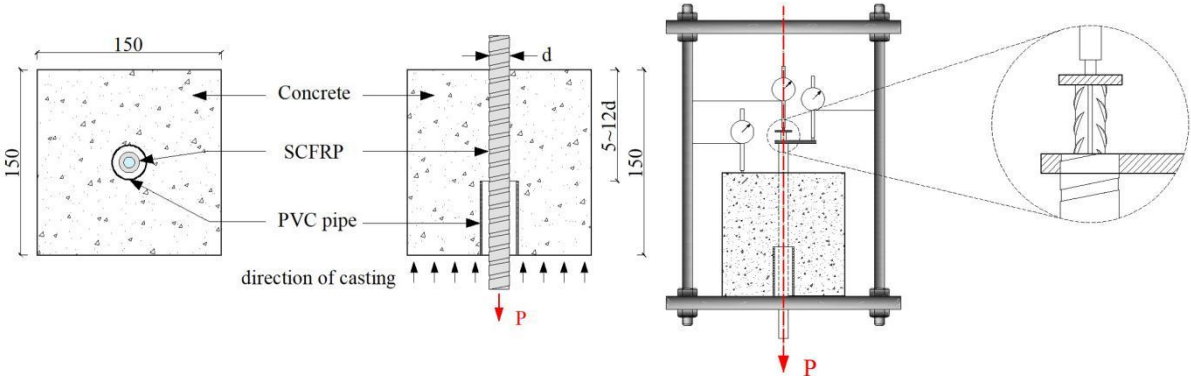


Figure 4 The schematic diagram of the specimens

**2.4 Pull out tests set up**

As shown in Figure 5, the loading rate of pull-out load is 0.75 mm/min, sampling frequency is 0.5 kN/time. An extensometer is arranged vertically on the surface of coral concrete to obtain slip data of concrete. Considering that the thickness of carbon fiber wrapped in SCFRP bar is thinner and the diameter of steel core is smaller, the micrometer probe has made a sleeve and sheet to measure slip data. The slip values of carbon fibers and steel cores are measured. For CFRP bar bonded specimens, it is not necessary to measure the slip value of steel core, other specimens are the same as SCFRP bar bonded specimens. When any of the following conditions occur during the test process, the test ends: (1) the steel bar breaks; (2) the coral concrete splits; (3) the free end slip exceeds 40 mm.



Note: P is the pulling force.

Figure 5 The schematic diagram of pull-out test equipment

**3. Test results analysis**

**3.1 Stress analysis of SCFRP bar and bond**

In the pull-out test, the diagonal extrusion force of FRP tendons can be decomposed into shear stress parallel to the bonding surface of tendons and concrete and radial force perpendicular to the bonding

surface of bonding performance between FRP tendons and concrete. The shear stress provides bonding force, while the radial force causes circumferential tensile stress of surrounding concrete, as shown in Figure 6(a). In the bonding between SCFRP bar and concrete, there are two bonding interfaces of "fiber and concrete, fiber and steel core", and steel core needs to transfer stress through carbon fiber. Therefore, under pull-out load, the mechanism of interface stress transfer and failure is more complex than that of single material steel bar, as shown in Figure 6(b).

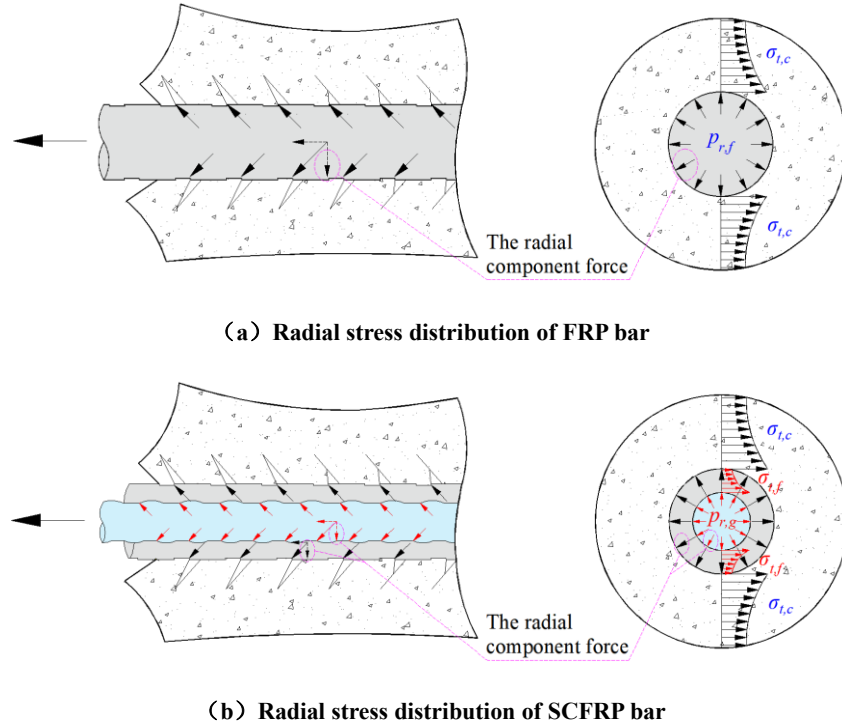


**Figure 6 Stress distribution of rebars**

Formula (1) is usually used to calculate the average bond stress between steel bar and concrete in central pull-out test. Although it is assumed that the stress distribution along the length direction is uniform, there is a inaccuracy in the prediction, but when bond length is relatively short (usually expressed by a multiple of the diameter of the reinforcement), it has sufficient accuracy:

$$\tau = \frac{P}{\pi d l_d} \quad (1)$$

Where ,  $\tau$  is the average bond strength (MPa);  $P$  is the pull-out force (kN);  $d$  is the diameter (mm) of SCFRP or CFRP bars;  $l_d$  is the bond length (mm) of SCFRP or CFRP bars.

If the bond between the fibers and the steel core is good and no relative slip occurs under the action of external forces, the tension between the fibers and the steel core is mainly determined by the elastic modulus of the material itself and the cross-sectional area. Therefore, neglecting the tension Poisson effect of steel bars, the tension of the two composites and the average bond stress at the two interfaces can be obtained by using the equal stiffness rule of composite materials.

$$F_s = F_{sf} \cdot \frac{E_s A_s}{E_s A_s + E_f A_f} \quad (2)$$

Substitute (2) into (1), rearrange, we can get:

$$\tau_1 = \frac{F_{sf}}{\pi d_{sf} l} \quad (3)$$

$$\tau_2 = \frac{F_s}{\pi d_s l} = \frac{F_{sf}}{\pi d_s l} \cdot \frac{E_s A_s}{E_s A_s + E_f A_f} \quad (4)$$

$$A_{sf} = \pi \left( \frac{d_{sf}}{2} \right)^2 = \frac{\pi}{4} d_{sf}^2 \quad (5)$$

$$A_s = \pi \left( \frac{d_s}{2} \right)^2 = \frac{\pi}{4} d_s^2 \quad (6)$$

$$A_f = A_{sf} - A_s = \frac{\pi}{4} (d_{sf}^2 - d_s^2) \quad (7)$$

Where,  $F_{sf}$ 、 $d_{sf}$ 、 $A_{sf}$  are the section load, section diameter and section area of SCFRP bars respectively;  $F_s$ 、 $d_s$ 、 $A_s$ 、 $E_s$  are the section load, stress, section diameter, section area and elastic modulus of SCFRP steel cores respectively;  $A_f$  and  $E_f$  are the section area and elastic modulus of SCFRP coated carbon fiber respectively;  $\tau_1$  is the bond between fiber and concrete interface.  $\tau_2$  is the bond strength between fiber and steel core;  $l$  is the bond length of steel bar.

If the strain hardening of the steel core is not considered, the tensile stress of steel core will not increase after yield. At this time, there is a theoretical maximum of bond stress at the bond interface between steel core and fiber, as shown in Figure 7.

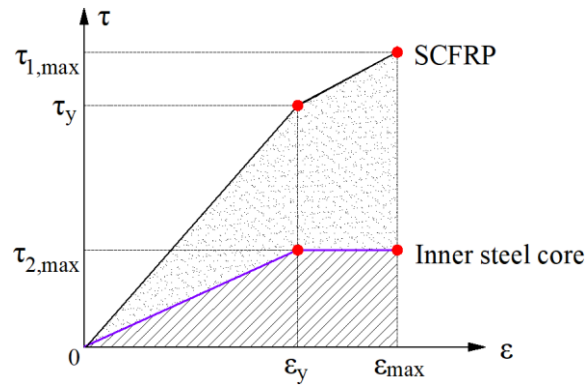


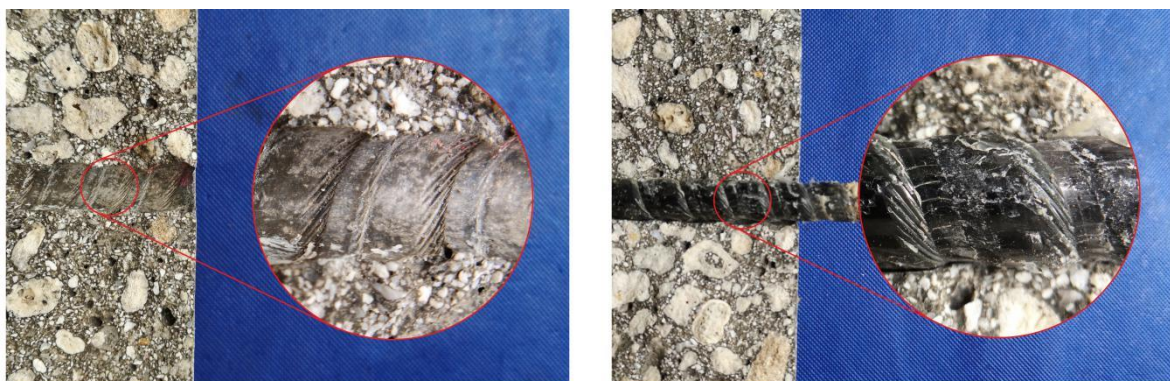
Figure 7 Bond stress strain relation of internal and external surface of SCFRP bar

### 3.2 Failure modes of bond

In the pull-out test of single material reinforcement, there are three kinds of failure: pull-out of reinforcement, fracture of reinforcement and splitting of concrete. For SCFRP bars, steel bar pull-out failure can be divided into steel core pull-out before yielding and steel core pull-out after yielding; concrete splitting failure can also be divided into coral concrete splitting before steel core yielding and coral concrete splitting after steel core yielding.

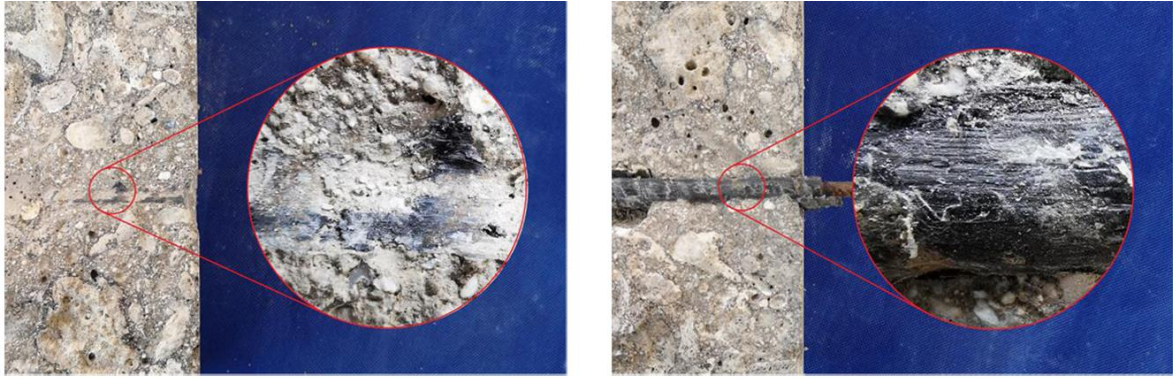
The production process determines that the diameter of SCFRP bars will not be too small. The larger diameter results in the smaller relative concrete thickness ( $c/d$ ) and the higher ultimate tensile strength of SCFRP bar itself. Therefore, coral concrete splitting occurs mainly before steel core yielding, and a small number of specimens occur steel bar pulling out and steel core yielding.

The SCFRP bar diameter of S12-5d shown in Figure 8(a) is 12 mm, the thickness of concrete cover is 69 mm ( $c/d=5.75$ ), and the bond length is 5d. The concrete is subjected to the radial compressive stress of SCFRP bar, which results in tensile stress. When the ultimate tensile stress of coral concrete is greater than that of coral concrete, coral concrete splitting occurs. The SCFRP transverse ribs on the cross section of the damaged coral concrete specimens are clear, and the surface and transverse ribs of the SCFRP bar specimens are only slightly worn, indicating that there is no obvious slip between the SCFRP bar and the coral concrete. The concrete protective layer thickness of S12-5d\* specimens shown in Figure 8(b) is 94 mm. Other conditions are the same as that of S12-5d specimens. Tendons are pulled out and damaged. The surface of SCFRP and its transverse ribs are severely worn and smoothed. Obvious friction marks at the bonding interface and shear damage on the surface of composite ribs can be observed on the split coral concrete blocks. Residual powder. The concrete cover thickness of S12-10d\* specimens shown in Figure 8 (c) is 94 mm and the bond length is 10d. The binding force provided by concrete is strengthened. When the tensile stress is greater than the yield stress of steel core and the ultimate tensile stress of coral concrete, the coral concrete splitting occurs after the yield of steel core. In addition to the SCFRP transverse rib marks, the epoxy resin debris left by the damaged ribs and a few carbon fiber marks left at the transverse ribs can also be seen on the section of the damaged specimens.



Note: The SCFRP transverse ribs on the cross section of the damaged coral concrete specimens are clear, and the surface and transverse ribs of the SCFRP bar specimens are only slightly worn.

(a) S12(6)-5d splitting of concrete before the yielding of the steel core



Note: Obvious friction marks at the bonding interface on the split coral concrete blocks, and the surface of SCFRP and its transverse ribs are severely worn and smoothed.

(b) S12(6)-5d\* pullout failure



Note: In addition to the SCFRP transverse rib marks, the epoxy resin debris left by the damaged ribs and a few carbon fiber marks left at the transverse ribs can also be seen on the section of the damaged specimens, and the surface and transverse ribs of the SCFRP bar specimens are moderately worn.

(c) S12(6)-10d\* splitting of concrete after the yielding of the steel core

Figure 8 Failure mode of Bond

### 3.3 Bond slip relationship

In the current research, bond-slip curve is usually used to reflect the bond performance between reinforcement and concrete. For the two failure modes of steel bar fracture and concrete splitting, it is difficult to get a complete line before the steel bar is pulled out. Based on the comprehensive analysis of references and the test results, the theoretical curves of SCFRP and coral concrete can be obtained, as shown in Figure 9.

- (1) **micro-slip stage**, at the initial stage of loading, the slip is very small, and the curve is nearly linear. At this time, the bonding force between SCFRP bar and coral concrete mainly comes from the chemical bonding force.
- (2) **slip stage**, the chemical bonding force between SCFRP bar and coral concrete gradually loses, and the main source of bonding stress changes into mechanical biting force and friction force. With the increase of pull-out load, the wedge effect between the cross ribs on the surface of SCFRP bar and the surrounding coral concrete makes the bonding strength of SCFRP bar and coral concrete increase

significantly. The increase of slip is accelerating, and the curve begins to show a non-linear feature. It should be specially pointed out that the curve of the slip stage can be divided into two sub-slip stages when the yield of steel core is taken as the inflection point. Because the elastic modulus of SCFRP bar decreases obviously because of the yield of steel core, the slope of the curve also decreases obviously. As the load continues to increase, the bond strength gradually approaches the ultimate bond strength, and the curve tends to the ultimate bond strength. It's gentle.

(3) **descending stage**, the bond stress decreases slowly in a short period of time, but with the weakening of wedge effect and the decreasing of friction force, the curve enters a rapid descending stage, and the slip increases sharply until the curve approaches the first stress trough bottom, i.e., the slip is close to a rib spacing of the fibers on the outer surface of SCFRP bar. The process of pulling out the transverse ribs. The main sources of bond stress at this stage are friction and partial mechanical occlusion.

(4) **residual stage**, the SCFRP transverse ribs are continuously sheared and worn, but the residual mechanical occlusion force and friction force can still provide a certain cohesive force. With the increase of slip, the cohesive stress rises and decreases. The curve shows a decline process of rising and falling, and the peak stress decreases gradually until the SCFRP bar is completely pulled out, and two adjacent peaks. Value spacing is approximately equal to one rib spacing of SCFRP.

For the S12-5d\* specimen shown in Fig. 10(a), the curve between SCFRP and coral concrete has complete micro-slip, slip, descent and residual stages. According to the ultimate load and curve of pull-out test, the failure mode of SCFRP is pull-out failure of steel core before yielding.

Figure 10 (b) shows the S12 (6) - 5d specimens. At the initial stage of loading, the fiber-concrete interface is in the micro-slip stage, and its line increases linearly with a slope of almost 0. With the increase of load, the fiber-concrete interface enters the slip section, and slips gradually until the coral concrete splits. During this period, SCFRP bar does not yield. The failure mode of the specimen is similar to that of the concrete splitting in the theoretical curve.

The initial loading curve of S12(6)-10d\* specimen shown in Figure 10(c) is similar to that of Figure 10(b). When the load increases to 6kN, the steel core yields and the slope of the curve decreases significantly. The steel core begins to enter the second sub-slip stage, and continues to load until the coral concrete splitting, which belongs to the splitting failure mode of concrete after the steel core yields. The theoretical curves are in good agreement.

The bond slip between SCFRP fibers and steel cores can also be expressed by curves. Figure 10 (b) and Figure 10 (d) are the bond-slip curves and load-slip curves of the splitting failure of steel core concrete of S12 (6) -5d specimens before yielding, respectively. The slip trend and value of steel core and fiber relative to coral concrete are basically the same, which are influenced by material characteristics and stress transfer mechanism. Under the same load conditions, steel core slip. The slip value of carbon fibers is only slightly smaller than that of carbon fibers, which indicates that the fibers and steel cores of the specimens maintain good bonding performance without obvious slip. Figure 10 (c) and Figure 10 (e) are the bond-slip curves and load-slip curves of concrete splitting failure after steel core yielding of S12 (6) - 10d\* specimens respectively. Before steel core yielding, the elastic modulus of SCFRP decreases, and the slope of load-slip curve of specimens begins to be lower than that before steel core yielding. The load-slip curves

of the bond interface between coral concrete and steel core remain close to each other. However, due to the redistribution of stress in steel core after yield, carbon fibers gradually bear more tensile stress, and the slip difference between them increases gradually, and the curve between fiber and steel core shows slip. It should be noted that the fiber and steel core have good bonding and overall mechanical properties during the pull-out test.

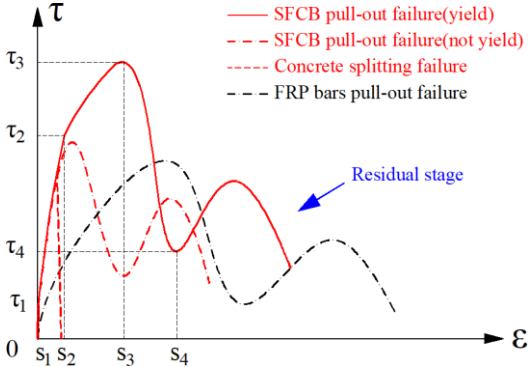
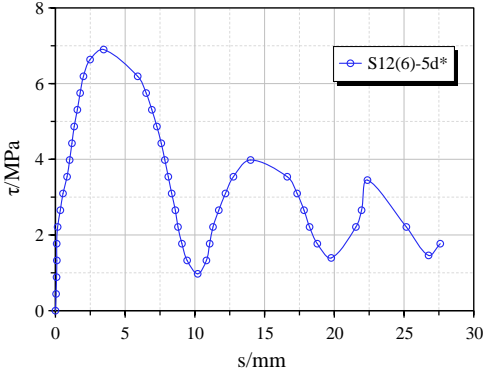
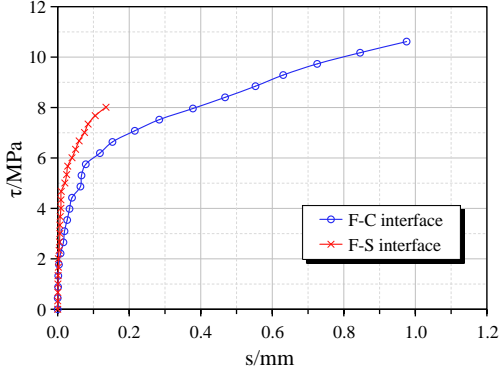
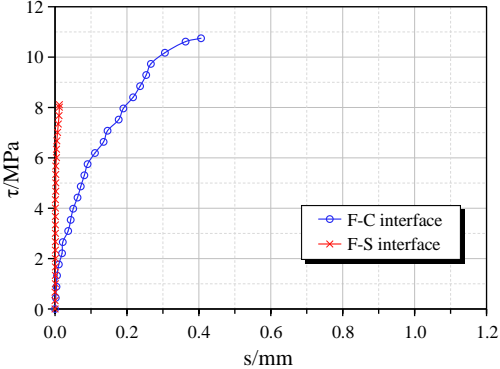


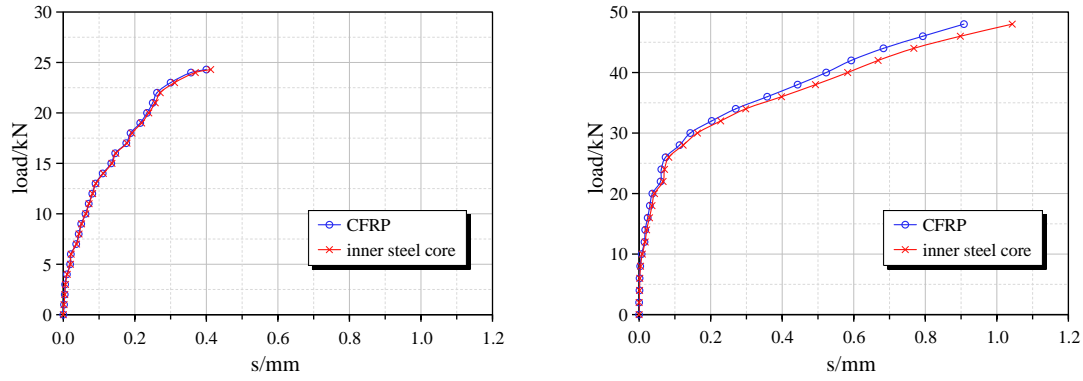
Figure 9 Theoretical  $\tau \sim s$  relationship



(a)  $\tau \sim s$  of S12(6)-5d\*



(b)  $\tau \sim s$  (Concrete splitting before steel core yielding) (c)  $\tau \sim s$  (Concrete splitting after steel core yielding)



(d)  $load \sim s$  (Concrete splitting before steel core yielding) (e)  $load \sim s$  (Concrete splitting after steel core yielding)

Figure 10  $\tau \sim s$  and  $load \sim s$  relationships

## 4. Key factors affecting the bond performance

### 4.1 Effect of SCFRP bar diameter and bond length

Figure 11 shows the effect of SCFRP bar diameter on bonding properties. With the increase of SCFRP bar diameter, the bond strength between SCFRP bar and coral concrete decreases, and the free end slip increases [32]. The larger the diameter of reinforcement, the smaller the relative bond area between reinforcement and concrete, which is the main reason for the reduction of bond strength. In addition, when the size of the specimen is fixed, the larger the diameter of the reinforcement, the smaller the relative thickness of the protective layer of the specimen, and the smaller the radial restraint that coral concrete can provide to SCFRP bar. FRP tendons are unidirectionally distributed fibers bonded by resin matrix and realize stress transfer between fibers. Therefore, the tensile stress on the cross section of the tendons is not uniformly distributed, but there is a certain stress lag phenomenon. Generally speaking, the strain of the outer fiber is slightly larger than that of the inner fiber. The larger the diameter, the more obvious the stress lag phenomenon is. Because the bond stress of FRP tendons distributes nonlinearly along the bond length, when the bond length is short, the high stress zone is relatively long and the average bond stress is relatively large, while when the bond length is long, the high stress zone is relatively short and the average bond stress is relatively small, so the average bond strength decreases with the increase of bond length. However, increasing the bond length between FRP bars and concrete can significantly increase the bond strength between FRP bars and concrete. As shown in Figure 12, the bond strength between SCFRP bar with a diameter of 12 mm and coral concrete increases from 24.3 kN in 5 days to 36.85 kN in 12 days. It is noteworthy that when the bond length of SCFRP bar increases to 10 days, the tensile stress of the steel bar has exceeded the yield stress of the steel core. With the yield of the steel core, the elastic modulus of SCFRP bar decreases, the slope of the curve decreases obviously.

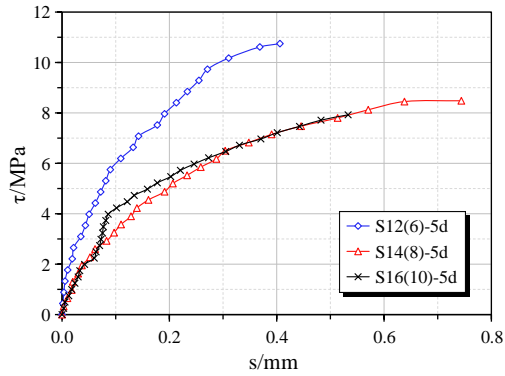


Figure 11 Effect of SCFRP diameter

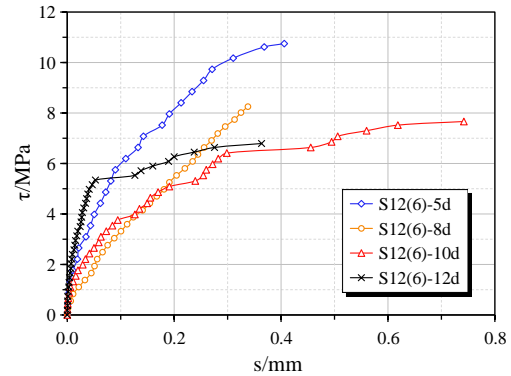


Figure 12 Effect of bond length SCFRP

## 4.2 Effect of Type of reinforcement

The type of reinforcement has a significant effect on the bonding performance, especially the surface condition and elastic modulus of the reinforcement. Without considering the surface condition of the steel bar, the greater the elastic modulus of the steel bar, the greater the slope of the rising section of the curve. Thanks to the high elastic modulus of steel, the elastic modulus of SCFRP bar increases to a certain extent. When the appearance conditions of steel bars are similar, the slope of curve rising section between SCFRP bar and coral concrete is larger than that of common FRP bars, as shown in Table 4 and Figure 13.

Table 4 Mechanical properties of rebars

Type of rebars	Nominal diameter /mm	Rib height /mm	Rib spacing /mm	Young's Modulus /GPa	Ultimate tensile strength /MPa	Cube compressive strength /MPa	Tensile splitting strength /MPa	Bond length /mm
GFRP bar	12	0.36	9.1	43	859	22.5	2.01	8d
BFRP bar		0.60	11.0	45	1250	36.3	2.98	5d
CFRP bar		0.70	8.6	114	1907.6	37.7	2.10	5d
SCFRP bar		0.50	11.0	127	760.4	37.7	2.10	5d

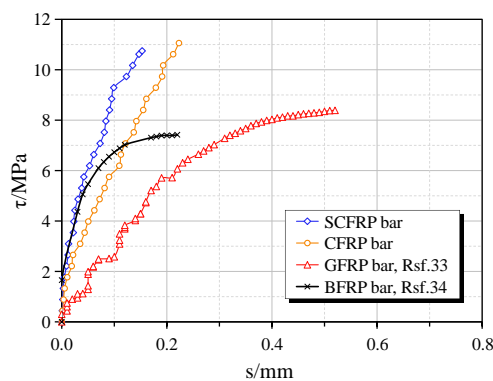


Figure 13 Effect of Type of rebars on  $\tau \sim s$  relationship

### 4.3 Effect of Coral concrete

Due to the influence of porous characteristics of coral debris aggregate, the porosity of coral concrete is much larger than that of ordinary concrete, which is the main reason that the strength and modulus of elasticity of coral concrete are lower than that of ordinary concrete under the same mix ratio [35-36]. Lower modulus of elasticity indicates that coral concrete has to produce greater strain to provide the same restraint stress as ordinary concrete, which is obviously not conducive to the bond between coral concrete and FRP bars. Therefore, the curve slope of SCFRP bar coral concrete is significantly smaller than that of SCFRP bar concrete. In addition, coral concrete at the interface with SCFRP bar is more likely to break and break when it is pressed and sheared, especially when SCFRP bar is pulled out. As shown in Figure 14, the average shear stress of SCFRP bar coral concrete bond pull-out specimens is less than that of ordinary concrete when the test conditions are relatively close.

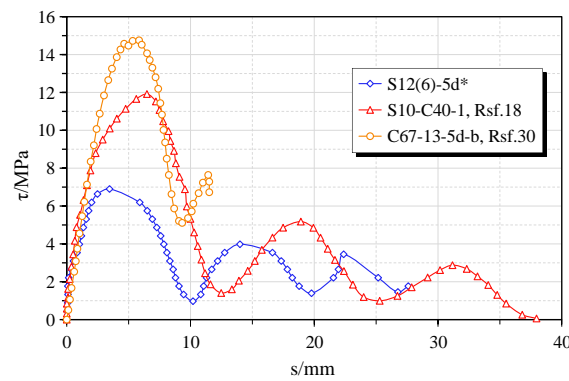


Figure 14  $\tau \sim s$  relationship between SCFRP bar coral concrete specimen and SCFRP bar ordinary concrete specimen

## 5. Bond slip model for this new type of concrete

At present, the bond-slip constitutive models of FRP tendons are mainly improved BPE model [23], Malvar model [24-25], CMR model [26], Zhang model [27], continuous curve model [28]. Based on the literature and experimental data, the stress process of SCFRP bar and concrete in bond-slip process is analyzed. It can be seen that the existing bond-slip constitutive model does not take into account the curve changes caused by steel core yield, and there is a big error with the actual test curve. The effect of steel core yield on the curve is very obvious. The curve is divided into four characteristic points: elastic slip point, steel core yield slip point, peak slip point and residual slip point. Based on the analysis of experimental curves and bond-slip mechanism, and on the basis of literature [30], a curve model is proposed in this paper, which describes the bond-slip constitutive relationship of the whole bond-slip process of steel core before and after buckling, respectively.

The bond-slip constitutive model of SCFRP bar-concrete is expressed as follows:

(1) When the steel core does not yield in the drawing test, the bond-slip constitutive model of SCFRP bar-concrete is expressed as follows:

$$\text{Micro slip stage: } \tau = \frac{\tau_1}{s_1} s \quad (s \leq s_1) \quad (1)$$

$$\text{Slip stage: } \frac{\tau}{\tau_2} = 2 \left( \sqrt{\frac{s}{s_2}} \right)^\alpha - \frac{s}{s_2} \quad (s_1 < s \leq s_2)$$

(2)

$$\text{Descending stage: } \tau = \tau_2 \frac{(s_3 - s)^2 (2s + s_3 - 3s_2)}{(s_3 - s_2)^3} + \tau_3 \frac{(s - s_2)^2 (3s_3 - 2s - s_2)}{(s_3 - s_2)^3} \quad (s_2 < s \leq s_3) \quad (3)$$

In the formulas,  $\tau$ 、 $\tau_1$ 、 $\tau_2$ 、 $\tau_3$  are theoretical bond strength, elastic bond strength, peak-valley bond strength, peak-valley bond strength respectively;  $s$ 、 $s_1$ 、 $s_2$ 、 $s_3$  are free-end slip value corresponding to measured free-end slip value, elastic bond strength, free-end slip value corresponding to peak-valley bond strength, peak-valley bond strength and the sliding value of the free end respectively;  $\alpha$  is determined by experiment.

(2) When the steel core yields in the pull-out test, the bond-slip constitutive model of SCFRP-concrete is expressed as follows:

$$\text{Micro slip stage: } \tau = \frac{\tau_1}{s_1} s \quad (s \leq s_1) \quad (4)$$

$$\text{Slip stage (before steel core yield): } \tau = (\tau_2 - \tau_1) \left( \frac{s - s_1}{s_2 - s_1} \right)^{0.86} + \tau_1 \quad (s_1 < s \leq s_2) \quad (5)$$

$$\text{Slip stage (after steel core yield): } \tau = (\tau_3 - \tau_2) \left( \frac{s - s_2}{s_3 - s_2} \right)^{1.0} + \tau_2 \quad (s_2 < s \leq s_3) \quad (6)$$

$$\text{Descending stage: } \tau = \tau_3 \frac{(s_4 - s)^2 (2s + s_4 - 3s_3)}{(s_4 - s_3)^3} + \tau_4 \frac{(s - s_3)^2 (3s_4 - 2s - s_3)}{(s_4 - s_3)^3} \quad (s_3 < s \leq s_4) \quad (7)$$

In the formulas,  $\tau$ 、 $\tau_1$ 、 $\tau_2$ 、 $\tau_3$ 、 $\tau_4$  are theoretical bond strength, elastic bond strength, yield point bond strength, peak-valley bond strength, peak-valley bond strength respectively;  $s$ 、 $s_1$ 、 $s_2$ 、 $s_3$ 、 $s_4$  are free-end slip value corresponding to measured free-end slip value, elastic bond strength and free-end slip value corresponding to yield point bond strength, the free-end slip value corresponding to the peak ultimate bond strength and the free-end slip value corresponding to the peak-valley bond strength respectively.

As shown in Figure 15, the curve model presented in this paper is in good agreement with the experimental data and can describe the stress process of SCFRP bar inner steel core before and after yielding. It needs to be pointed out that there are few experimental data on the bond performance between

SCFRP bar and concrete at present. The applicability and accuracy of the model proposed in this paper need to be further verified by a large number of experimental data.

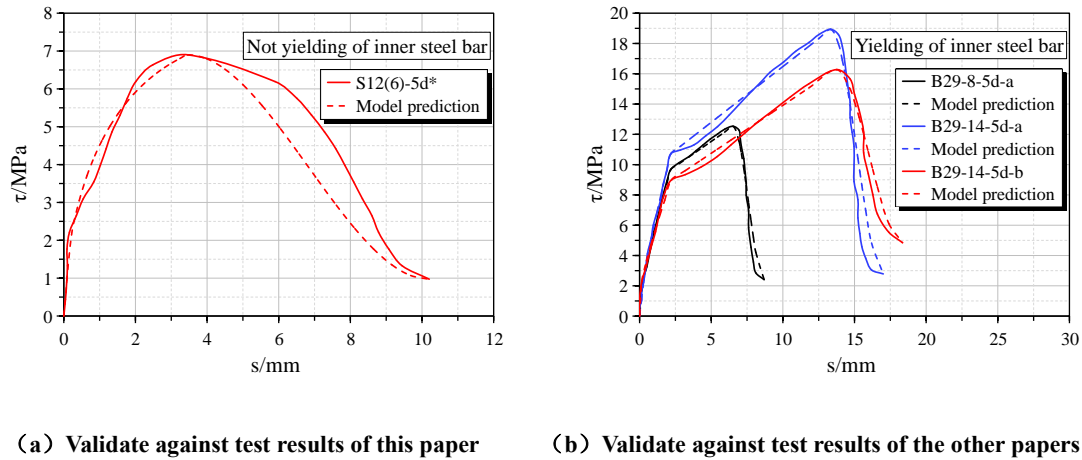


Figure 15 Validation of proposed  $\tau \sim s$  model

## 6. Conclusion

(1) The failure mode and mechanism of bond-slip between SCFRP bar and coral concrete are more complex than that of single material reinforcement. Although the pull-out specimens still show three failure modes: steel pull-out, steel fracture and concrete splitting, the failure modes of steel pull-out can be subdivided into steel core pull-out before yielding and steel core pull-out after yielding; concrete splitting failure modes can also be divided into coral concrete splitting before steel core yielding and after steel core yielding.

(2) The curves of SCFRP bar and coral concrete bond specimens are divided into two sub-slip stages at the slip stage, with the steel core yield as the inflection point. The elastic modulus of SCFRP bar decreases obviously after the steel core yield, and the slope of the curve decreases obviously, and the curve becomes smoother. There are elastic slip points, steel core yield slip points and peak slip in the curves.

(3) The factors affecting the bonding performance of SCFRP bar coral concrete are similar to FRP bar concrete. When test conditions are the same, with the increase of SCFRP bar diameter, the bond strength between SCFRP bar and coral concrete decreases. The bond strength of specimen with diameter of 16mm decreased by 26.3% than that of specimen with diameter of 12mm. With the increase of bond length, the bond strength between SCFRP bar with a diameter of 12 mm and coral concrete increases from 24.3 kN in 5 days to 36.85 kN in 12days, but the average bond strength decreases by 36.8%.

(4) When bonding specimens and test conditions are similar, the bonding performance between SCFRP and coral concrete is lower than that of ordinary concrete, and the ultimate bond strength is 50% of ordinary concrete. The relative slip between SCFRP bar and coral concrete is earlier than that of ordinary concrete, and the amount of slip is larger.

(5) The bond slip model of SCFRP reinforced coral concrete was developed with the coefficients of slip (before steel core yields) and slip after steel core yields are 0.86 and 1.0 respectively, which can describe the

bond slip behavior between SCFRP and concrete more accurately.

The future research will be considered from the following aspects: including using different test methods (such as: Pull-out test、 Beam test, etc.), different loading methods (such as: Uniaxial tension、 Cyclic tension、 Repeated tension,etc.) and different reinforcement materials(such as: SGRFP、 SBRFP, etc.). In order to establish the design calculation theory more systematic and complete.

## Acknowledgements

This paper is supported by the National Natural Science Foundation of China (51868014), the High-Level Innovation Team in Colleges and Universities and Excellence Scholar Program" Island and Coastal Environment Concrete Structure "in Guangxi (in 2017) and Innovation-driven Development Project "Development and Demonstration of High-Erosion Construction Materials in Complex Marine Environment" in Guangxi(in 2018). The views expressed are the authors' alone.

## Reference

- [1] Ehlert Rick A. Coral Concrete at Bikini Atoll. *Concrete International*, 1991, (1):19-24.
- [2] Lee S C. Prediction of concrete strength using artificial neural networks. *Engineering Structures*, 2003, 25(7):849-857.
- [3] W. Yodsudjai, N. Otsuki, T. Nishida, et al. Study on strength and durability of concrete using low quality coarse aggregate from circum-pacific region, in: Fourth Regional Symposium on Infrastructure Development in Civil Engineering (RSID4), 2003, pp:171-180.
- [4] WANG Lei, ZHAO Yan-lin, LÜ Hai-bo. Prospect on the properties and application situation of coral aggregate concrete[J]. *Concrete*, 2012(2):99-100+113.G.(in Chinese)
- [5] Tomlinson D, Fam A. Performance of Concrete Beams Reinforced with Basalt FRP for Flexure and Shear[J]. *Journal of Composites for Construction*, 2015, 19(2):04014036.
- [6] Zhiqiang Dong, Gang Wu, Xiaoling Zhao, Jindong Ling. Long-Term bond durability of Fiber-reinforced polymer bars embedded in seawater sea-sand concrete under ocean environments[J]. *Composites for Construction*, 2018, 22(10).
- [7] Zhiqiang Dong, Gang WU, Hong ZHU. Mechanical properties of seawater sea-sand concrete reinforced with discrete BFRP-Needles[J]. *Construction and Building Materials*, 2019, 206(5):432-441.
- [8] Burong Zhang, Brahim Benmokrane, Member, ASCE and Adil Chennouf. Prediction of Tensile Capacity of Bond Anchorages for FRP Tendons. *Journal of Composites for Construction*. 2000, 4(05).
- [9] Marta Baena, Lluís Torres, Albert Turon. Cristina Barris Experimental study of bond behaviour between concrete and FRP bars using a pull-out test. *Composites: Part B*. 2009, 40(07):784-797.
- [10] Fei Li, Qi Lin Zhao, Hao Sen Chen, Jin Quan Wang, Jing Hui Duan. Prediction of tensile capacity based on cohesive zone model of bond anchorage for fiber-reinforced polymer tendon. *Composite Structures*. 2010, 92(03):2400-2405.
- [11] Kim Y J , Siriwardanage T , Hmidan A , et al. Material characteristics and residual bond properties of organic and

- inorganic resins for CFRP composites in thermal exposure. *Construction and Building Materials*, 2014, 50:631-641.
- [12] Ghiassi, Bahman, Paulo B. Lourenço, and Daniel V. Oliveira. "Accelerated hygrothermal aging of bond in FRP - masonry systems." *Journal of Composites for Construction*, 2014,19( 3 ).
- [13] Seo, J.W., Kim Y.J., and Zandyavari S. Response surface Metamodel-based performance reliability for reinforced concrete beams Strengthened with FRP Sheets. *Special Publication* , 2015, 304: 1-20.
- [14] Wang L , Mao Y , Lv H , et al. Bond properties between FRP bars and coral concrete under seawater conditions at 30, 60, and 80°C[J].*Construction and Building Materials*,2018,162:442-449.
- [15] Bank L C. Progressive Failure and Ductility of FRP Composites for Construction:Review.*Journal of Composites for Construction*.2013,17(3):406-419.
- [16] Ovitigala T, Ibrahim M A and Issa M A. Serviceability and Ultimate Load Behavior of Concrete Beams Reinforced with Basalt Fiber-Reinforced Polymer Bars.*ACI Structural Journal*.2016,113,757-768.
- [17] Nanni A, Henneke M J, Okamoto T. Tensile Properties of Hybrid Rods for Concrete Reinforcement[J].*Construction and Building Materials*.1994,8(1):27-34.
- [18] G Wu, Z Y Sun, Z S Wu and Y B Luo. Mechanical Properties of Steel-FRP Composite Bars (SCFRPs) and Performance of SCFRP Reinforced Concrete Structures[J].*Advances In Structural Engineering*.2012,15(04):625-635.
- [19] Q Hao, Y Wang, J Hou, J Ou. Bond-slip constitutive model between GFRP/Steel wire composite rebars and concrete[J].*Engineering mechanics*,2009,26(05):62-72.(in Chinese)
- [20] Eligehausen R, Popov E P and Bertero V V. Local bond stress-slip relationships of deformed bars under generalized excitations ,Rep No.83,Earthquake Engrg Ctr(EERC),Univ of California,Berkeley,Calif,1983.
- [21] Ehsani M R, Saadatmanesh H, Tao S. Bond Behavior of Deformed GFRP Rebars.*Journal of Composites Materials*,1997,14:1413-1430.
- [22] Ehsani M R, Saadatmanesh H, Tao S. Bond of Hooked Glass Fiber Reinforced Plastic (GFRP) Reinforcing Bars to Concrete.*ACI Materials Journal*.1995,92(4):391-400.
- [23] Cosenza E, Manfredi G, Realfonzo. Behavior and modeling of bond of FRP rebars to concrete[J].*Journal of Composites for Construction*,1997:40-51(2).
- [24] Malvar L J, Cox J V and Cochran K B. Bond between Carbon Fiber Reinforced Polymer Bars and Concrete I:Experimental Study.*Journal of Composites for Construction*.2003,7(2):154-163.
- [25] Malvar L J, Joshi N R, Beran J A and Novinson T. Environmental Effects on the Short-term Bond of Carbon Fiber-Reinforced Polymer (CFRP) Composites.*Journal of Composites for Construction*.2003,7(1):58-63.
- [26] Cosenza E, Manfredi G and Realfonzo R. Development Length of FRP Straight Rebars.*Composites Part B:Engineering*.2002,33:493-504.
- [27] Zhang B, Benmokrane B and Chennouf A. Prediction of Tensile Capacity of Bond Anchorages for FRP Tendons. *Journal of Composites for Construction*.2000,4(2):39-47.

- [28] Gao D, Zhu H, Xie The Constitutive Models for Bond-slip Relation Between FRP Rebars and concrete[J].Industrial Construction.2003(07):41-43+82.(in Chinese)
- [29] ZHENG Q, XUE W. Constitutive Relationship of Bond-slip Behavior of Sand-Coated Deformed GFRP Rebars.Engineering Mechanics.2008(09):162-169.(in Chinese)
- [30] Zhang Lin-lin. Study on Bond Behavior between Steel-FRP Composite Bar (SCFRP) and Concrete under Cyclic Loading[D].Southeast University,2011.
- [31] Zhi-qiang Dong, Gang Wu, Xiao-Ling Zhao, Hong Zhu and Jin-long Lian. Bond durability of steel-FRP composite bars embedded in seawater sea-sand concrete under constant bending and shearing stress.Construction and Building Materials.2018,192(10):808-817.
- [32] Baena M , Lluís Torres, Turon A , et al. Experimental study of bond behaviour between concrete and FRP bars using a pull-out test[J]. Composites Part B: Engineering,2009,40(8):784-797.
- [33] Wang Lei, Mao Yadong, Chen Shuang, Li Wei, Gu Wenhui. Experimental Research on Bond Performance between GFRP Bars and the Coral Concrete[J].Journal of Building Materials.2018,21(02):286-292.(in Chinese)
- [34] Yang Chao, Yang Shu-tong, Qi De-hai. Experimental Study on The Bond Performance between GFRP Bars and Coral Concrete[J].Engineering Mechanics.2018,35(S1):172-180.(in Chinese)
- [35] Li Y T , Zhou L , Zhang Y , et al. Study on Long-Term Performance of Concrete Based on Seawater, Sea Sand and Coral Sand[J]. Advanced Materials Research,2013,706-708(1):512-515.
- [36] Da B, Yu H, Ma H, Tan Y, M R, Dou X. Experimental investigation of whole stress-strain curves of coral concrete[J]. Construction and Building Materials,2016,122:81-89.